Sensors and Materials, Vol. 30, No. 5 (2018) 1123–1132
MYU Tokyo

S & M 1569

Nitric Oxide Gas Sensors Using Multilayered Thin Film with Interspaces

Akihiro Shimizu, Tsubasa Morita, Tomiharu Yamaguchi,* and Kazuhiro Hara

Graduate School of Engineering, Tokyo Denki University,
5 Senju-Asahi-cho, Adachi-ku, Tokyo 120-8551, Japan

(Received December 4, 2017; accepted April 10, 2018)

Keywords: NO gas sensor, WO_3 thin film, Ag catalyst, interspace, multiple-layered configuration

Nitric oxide (NO) is an air pollutant known to adversely affect the environment, humans, and other living organisms. Low-level NO gas is also created by human bodies and emitted as a component of exhaled breath and skin gas under some health conditions. Therefore, there is a strong demand for the monitoring of NO gas concentration. In this paper, we present novel NO gas sensors that have been developed using multilayered WO_3-based thin films with interspaces. Ag doping into a WO_3 thin film is effective in increasing the sensitivity to NO. Multilayered thin-film sensors with interspaces successfully enhance both sensitivity and selectivity to NO. The developed sensor with quadruple-layered sensing films can detect as low as 0.5 ppm NO gas with good selectivity at an operating temperature of 290 °C. The response and recovery times are 81 and 138 s, respectively, for the double-layered sensor, while its sensitivity is lower than that of the quadruple-layered sensor. Thus, the sensors are promising as a portable and inexpensive NO sensing device in various application fields such as environmental monitoring and health diagnosis.

1. Introduction

Nitric oxide (NO) is a harmful gas, which is generated by internal combustion engines, thermal power plants, industrial furnaces, and boilers and emitted as a component of exhaust gas.(1) It reacts with oxygen and moisture in the air to form HNO_2, which falls as acid rain. It causes photochemical smog and destroys the ozone layer.(2) In addition, it is an important cellular signaling molecule in humans and animals involved in many physiological and pathological processes. Low-level NO gas is also created by human bodies and emitted as a component of exhaled breath and skin gas under some health conditions. It is known that the exhaled air from patients suffering from asthma includes higher levels of NO. Therefore, the monitoring of NO gas concentration has attracted attention in various fields.

The concentration of NO in air can be determined by a chemiluminescent technique. The Saltzman method using the Griess-Saltzman reaction is also widely adopted. However, both methods require large and expensive equipment. Thus, there is a need for inexpensive

*Corresponding author: e-mail: t-yama@mail.dendai.ac.jp
http://dx.doi.org/10.18494/SAM.2018.1836

ISSN 0914-4935 © MYU K.K.
http://myukk.org/

and portable sensors in various fields. Although semiconductor gas sensors as well as electrochemical sensors have been developed to determine the concentration of NO,[3–7] in general, they are poor at distinguishing NO from NO_2.

In this paper, we present novel semiconductor thin-film NO gas sensors using a WO_3-based sensing film and a Ag catalyst with a multilayer configuration and interspaces between the sensing films. The WO_3-based material is sensitive to NO_x.[8–12] Ag doping into the WO_3 thin film is effective in increasing the sensitivity to NO.[13,14] A multilayered thin film with interspaces[15] successfully enhances both sensitivity and selectivity to NO.

2. Sensor Configuration and Materials

Two types of sensors have been developed and examined. The first one is a metal-oxide thin-film sensor without interspaces. The second one is a metal-oxide multilayered sensor with interspaces. The former has been fabricated to find effective materials and catalysts for detecting NO. The latter has been exploited to investigate the best configuration for a multilayered thin-film sensor with interspaces.

2.1 Thin-film sensors without interspaces

Figure 1 shows the configuration of a metal-oxide thin-film gas sensor. This sensor was also used as a reference sample. The substrate used was alumina and its dimension was $10 \times 10 \times 1$ mm^3. The sensing film has a double-layered structure without interspaces. The material for the first layer of the sensing film was Fe_2O_3 + TiO_2 (5 mol%) + MgO (4 mol%); TiO_2 was doped to increase the electron concentration in the Fe_2O_3 film, decreasing the sensor resistance while MgO was added to improve the stability of the film. The material for the second layer was WO_3 + Ag; Ag was doped to the WO_3-based film to increase the sensitivity to NO. Four kinds of sensors were fabricated with different Ag doping amounts of 2, 1, 0.5, and 0 wt% (nondoped). The active area of the sensing film was about 1×1 mm^2 and the thickness of both the first and second layers was 100 nm.

In general, WO_3-based films are more sensitive to NO than Fe_2O_3-based ones. However, WO_3-based films tend to often generate cracks during operation and thus the resistance of the films gradually increases with time. The bandgap of the Fe_2O_3-based film (ca. 2.3 eV) is

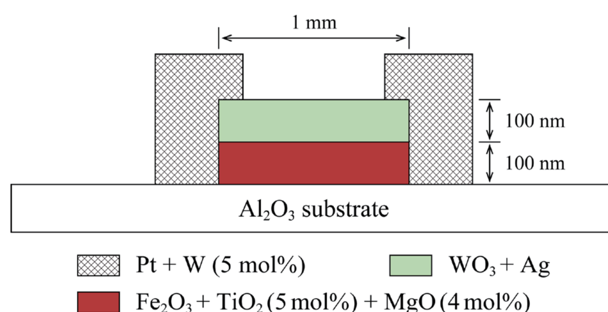

Fig. 1. (Color online) Cross-sectional view of a thin-film gas sensor without interspaces.

smaller than that of the WO_3-based one (ca. 2.8 eV). By using a double-layered configuration, most electrons flow in the Fe_2O_3-based film with a smaller bandgap.[16] The Fe_2O_3-based film seldom generates cracks, while possible cracks in the WO_3-based film do not have an adverse effect on the sensor resistance. Moreover, the α-type Fe_2O_3-based film has the same crystalline structure of corundum type as that of the alumina substrate. Hence, the adhesion of the Fe_2O_3-based film to the alumina substrate is good. In addition, the thermal expansion coefficient of the Fe_2O_3-based film is close to that of the alumina substrate. Thus, the internal stress associated with temperature rise inside the Fe_2O_3-based film is small, reducing the generation of cracks.

The material for the electrode was Pt + W (5 mol%); W was doped to enhance the durability of the Pt film. The thickness of the electrode was 200 nm. All the films were deposited by RF sputtering. The sputtering conditions are summarized in Table 1. All the target materials were of analytical grade. Photolithography was used to define the sensor and electrode geometries. The films were thermally treated at 600 °C for 5 h in air to allow for the recovery from various defects and the stabilization of the crystal structure.

2.2 Multilayered sensors with interspaces

Figure 2 shows the configuration of a multilayered metal-oxide thin-film gas sensor with interspaces. The substrate was alumina and its dimension was 10 × 10 × 1 mm^3. The sensing

Table 1
Sputtering condition.

	$Fe_2O_3 + TiO_2 + MgO$	WO_3 + Ag	SiO_2, $SiO_2 + Al_2O_3$	Pt + W
Sputtering target	Mixed powder of Fe_2O_3 (91 mol%), TiO_2 (5 mol%), and MgO (4 mol%)	Mixed powder of WO_3 and Ag	Small pieces of Al_2O_3 on a disc of SiO_2	Small sheets of W on a sheet of Pt
Sputtering atmosphere	Ar (80%) and O_2 (20%)	Ar (80%) and O_2 (20%)	Ar (80%) and O_2 (20%)	Ar (100%)
Power density	12 W/cm^2	12 W/cm^2	12 W/cm^2	12 W/cm^2

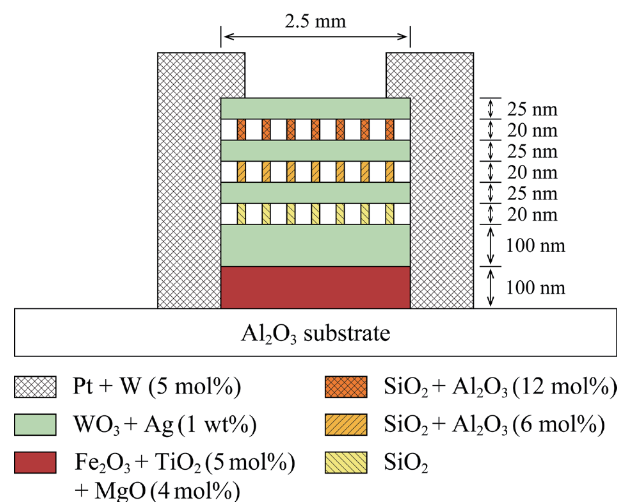

Fig. 2. (Color online) Cross-sectional view of a triple-layered thin-film gas sensor with interspaces.

film has a quadruple-layered structure with interspaces. The first and second layers of the sensing film are Fe_2O_3 + TiO_2 (5 mol%) + MgO (4 mol%) and WO_3 + Ag, respectively. The third to eighth layers are SiO_2, WO_3 + Ag (1 wt%), SiO_2 + Al_2O_3 (6 mol%), WO_3 + Ag (1 wt%), SiO_2 + Al_2O_3 (12 mol%), and WO_3 + Ag (1 wt%), respectively. The thicknesses of the third to eighth layers are 20, 25, 20, 25, 20, and 25 nm, respectively. The films were thermally treated at 600 °C for 5 h in air. The morphology of the WO_3-based films changed after this heat treatment from dense to porous, which enabled the sacrificial etching of SiO_2-based films through microscopic pores of the WO_3-based films.[15] Then SiO_2 + Al_2O_3 (12 mol%), SiO_2 + Al_2O_3 (6 mol%), and SiO_2 layers were partly dissolved with 1% fluoric acid, leaving pillars that supported the upper and lower WO_3-based films.

In the etching process, fluoric acid first penetrates through the top sensing film, next dissolves the upper sacrificial layer, then penetrates through the upper middle sensing film, next dissolves the middle sacrificial layer, then penetrates through the lower middle sensing film, and finally dissolves the lower sacrificial layer. In this process, the dissolution rates of the upper and middle sacrificial layers made of SiO_2 + Al_2O_3 (12 mol%) and SiO_2 + Al_2O_3 (6 mol%) were low and thus supporting pillars were sufficiently thick even after a prolonged etching process. The dissolution rate of the lower sacrificial layer made of SiO_2 was high and thus enough interspaces were formed. The measured dissolution rates were 4.8, 3.0, and 3.6 nm/min for SiO_2, SiO_2 + Al_2O_3 (6 mol%), and Al_2O_3 (12 mol%) films deposited on sapphire substrates, respectively. In our previous work, SiO_2 layers without Al_2O_3 were used as sacrificial layers between the WO_3-based layers.[15] In that case, the upper supporting pillars were very thin or removed after prolonged etching time. Thus, the sensor was fragile and easy to break. In this study, the dissolution rate was controlled by adding Al_2O_3 to the SiO_2 film to form wide interspaces as well as thick pillars.

The active area of the sensing film was about 2.5 × 2.5 mm^2. 1 wt% Ag was also doped to the WO_3-based film. The electrode was Pt + W (5 mol%) and its thickness was 200 nm. All the films were deposited by RF sputtering. The sputtering conditions were the same as those described in Table 1. Photolithography was used to define the sensor and electrode geometries. The films were thermally treated at 600 °C for 5 h in air to allow for the recovery from various defects and the stabilization of the crystal structure.

Triple-layered and double-layered sensors were also fabricated by a similar process for comparison with the quadruple-layered one in terms of the sensitivity to NO gas and the response and recovery times.

The surface morphologies of a WO_3-based film after annealing at 600 °C and subsequent etching by diluted fluoric acid are shown in Figs. 3(a) and 3(b), respectively. These photographs were taken by SEM (JEOL, JSM-6010PLUS/LA). The sensing film itself was porous with granular structures of about 100 nm diameter before etching, while possible microscopic pores are not clearly observed. The film exhibited many pores after etching, through which the underlying SiO_2-based film was dissolved. Our previous work shows pillars under the uppermost WO_3-based film by using an optical microscope (Keyence, VH-Z500).[15] As the WO_3-based film was transparent, SiO_2 pillars were clearly visible through the film.

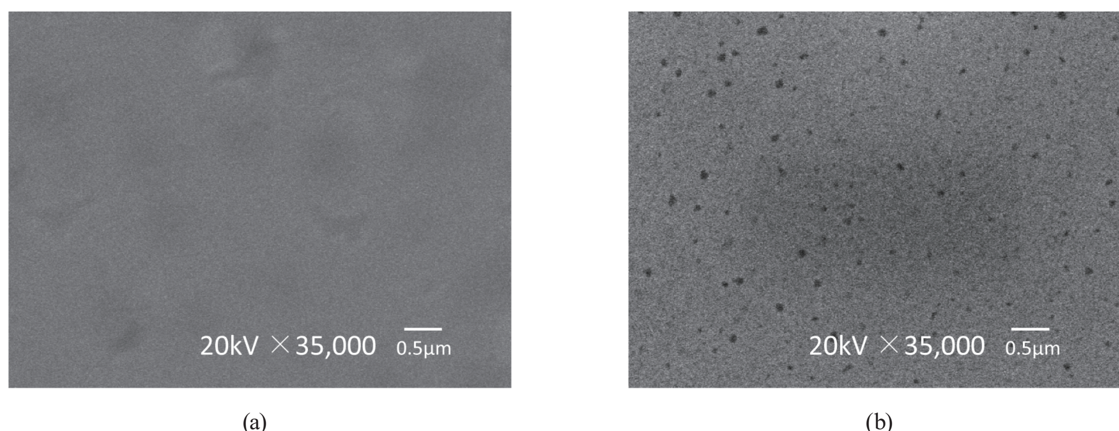

(a) (b)

Fig. 3. SEM images of a double-layered WO_3-based thin film: (a) after annealing at 600 ℃ and (b) after subsequent etching with diluted fluoric acid.

3. Experimental Results and Discussion

The sensors were tested in a closed test box (Figaro Engineering, SR-3) made of polymethylmethacrylate (PMMA). Its volume was 5.4 L. The sensors were heated to 100–400 ℃ by using a commercially available Pt heater covered with alumina. The experimental setup is shown in Fig. 4. Varous test gases were injected by a syringe. After the sensor resistance reached a steady value, the lid was opened to extract the test gases. NO, NO_2, NH_3, and SO_2 gases were taken from the gas cylinders (Taiyo Nippon Sanso) containing 1000 ppm NO, 200 ppm NO_2, 1000 ppm NH_3, and 200 ppm SO_2, respectively. All these gases were balanced with nitrogen. CO, CO_2, and H_2 gases were taken from the gas cylinders (Taiyo Nippon Sanso) containing standard gases with 99.9% purity. The NO gas concentration in the test box ranged from 0.1 to 10 ppm. The ambient temperature was about 23 ℃ and the relative humidity ranged from 26 to 45%RH.

3.1 Effect of Ag doping into WO_3-based film for the sensors without interspaces

The effect of Ag doping into the WO_3-based film was studied for the sensors without interspaces. The Ag doping amounts were 0.5, 1, 2, and 0 wt% (nondoped). NO gas concentration was fixed at 5 ppm. Figure 5 shows the temperature dependence of the sensitivity of the sensors with different Ag doping amounts. Here, the sensitivity S is defined as the ratio of the resistance in the gas, R_g, to that in the ambient air, R_a.

$$S = \frac{R_g}{R_a} \tag{1}$$

All the sensors doped with Ag exhibited higher sensitivity to NO gas than the nondoped sensor. The sensor doped with 1 wt% Ag showed the highest sensitivity and its sensitivity

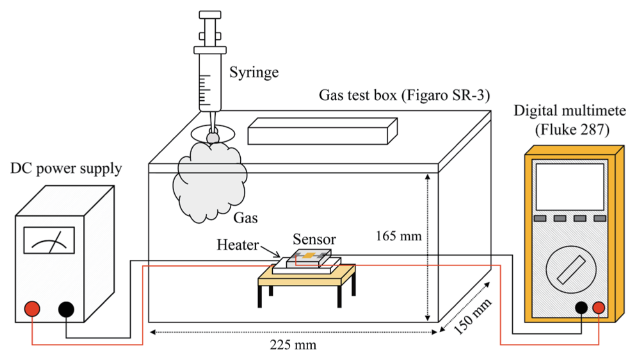

Fig. 4. (Color online) Experimental setup.

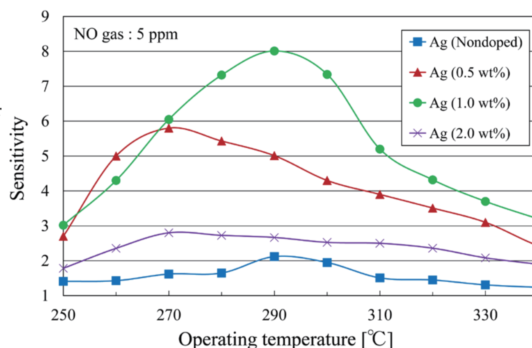

Fig. 5. (Color online) Dependence of sensitivity on operating temperature for gas sensors without interspaces with different Ag doping amounts into WO_3.

became maximum at an operating temperature of 290 °C. The experiments revealed that the doping amount of 1 wt% Ag into the WO_3 film was the best for NO detection.

3.2 Effect of wet etching time of sacrificial SiO_2 layers for the sensors with interspaces

The effect of the wet etching time of sacrificial SiO_2 layers for the sensors with interspaces was investigated. The double-layered, triple-layered, and quadruple-layered sensors were used in this experiment. The sensitivity to NO gas was measured at an operating temperature of 290 °C. The NO gas concentration was 5 ppm. Figure 6 shows the dependence of the sensitivity on the wet etching time of the sacrificial SiO_2 layers.

For the double-layered sensor, the maximum sensitivity to NO gas was obtained at the etching time of 7 min, while for the quadruple-layered sensor, the maximum sensitivity was obtained at the etching time of 20 min. The sensitivity to NO gas is higher for the quadruple-layered sensor than for the double-layered and triple-layered sensors regardless of etching time owing to the higher total surface area of the WO_3-based sensing films.

3.3 Dependence of the sensitivity on the NO concentration in air of the multilayered thin-film sensors with interspaces and that without interspaces

Figures 7(a) and 7(b) show the dependence of the sensitivity on NO concentration for the quadruple-layered and double-layered sensors with interspaces as well as that without interspaces in the lower (0.1 to 1 ppm) and higher (1 to 10 ppm) concentration range, respectively. The sensitivity of the multiple-layered sensors with interspaces is higher than that of the sensor without interspaces above 1 ppm. The sensitivity of the double-layered sensor is slightly higher than that of the quadruple-layered sensor below 1 ppm. This is due to the slow response of the quadruple-layered sensor compared with that of the double-layered sensor because the NO gas diffusion into the inner sensing films takes more time for the quadruple-layered sensor. From Fig. 7(a), it was clear that the double-layered and quadruple-layered sensors can detect as low as 0.5 ppm NO gas.

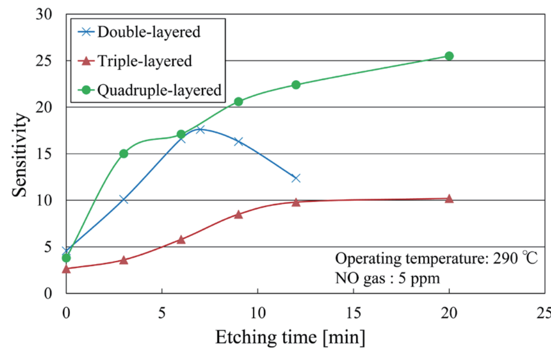

Fig. 6. (Color online) Dependence of sensitivity on etching time of sacrificial SiO_2 layers of multilayered gas sensors with interspaces.

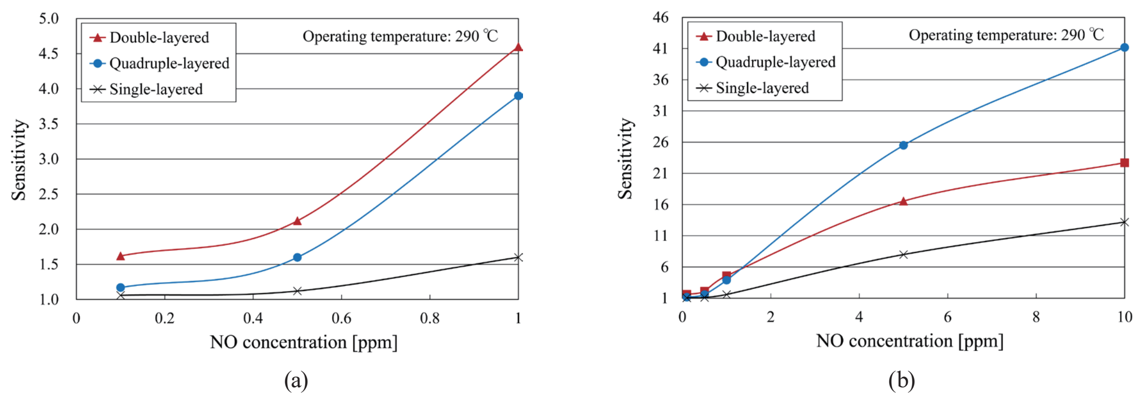

Fig. 7. (Color online) Dependence of sensitivity on NO concentration of multiple-layered gas sensors with interspaces as well as that without interspaces in (a) the lower and (b) higher NO concentration ranges.

3.4 Response and recovery times of the multilayered sensors with interspaces

The response and recovery times to NO gas were examined. Figure 8 shows the transient response toward NO gas for the double-layered (a) and quadruple-layered (b) gas sensors. The operating temperature was 290 °C and the gas concentration was 1 ppm. The response and recovery times were defined as the time for the resistance to reach a 90% change. The response and recovery times are 81 and 138 s for the double-layered sensor, while they are 244 and 599 s for the quadruple-layered sensor, respectively. These results revealed that the double-layered sensor had faster response and recovery characteristics, although it showed less sensitivity to NO gas at higher concentrations above 1 ppm. The slower response and recovery for the quadruple-layered sensor are possibly due to the slow diffusion of NO gas into and from the inner interspaces as mentioned earlier.

3.5 Gas selectivity of the double-layered sensor with interspaces

The sensitivity to various gases for the double-layered sensor with interspaces is shown in Fig. 9. The operating temperature was 290 °C. For the NH_3, CO, CO_2, and H_2 gases, the sensitivity S is defined as the ratio of the resistance in ambient air, R_a, to that in gas, R_g, as shown in the following, while for the other gases, it is defined as Eq. (1).

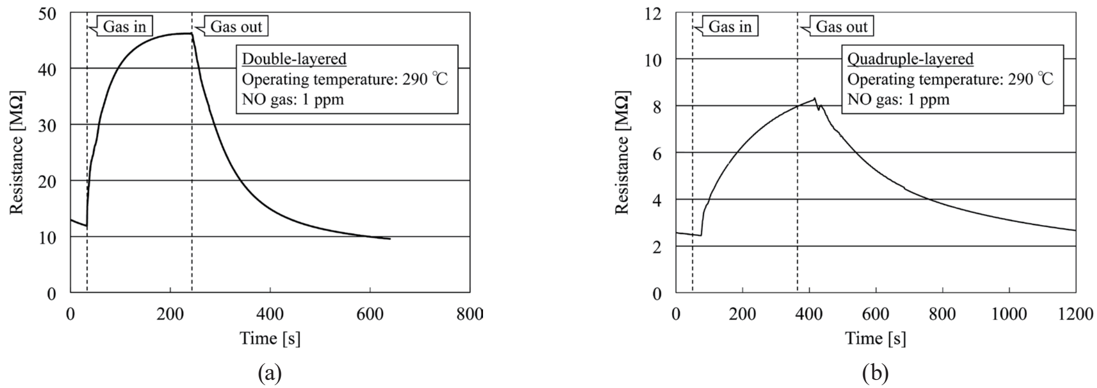

Fig. 8. Transient responses to NO of (a) double-layered and (b) quadruple-layered gas sensors with interspaces.

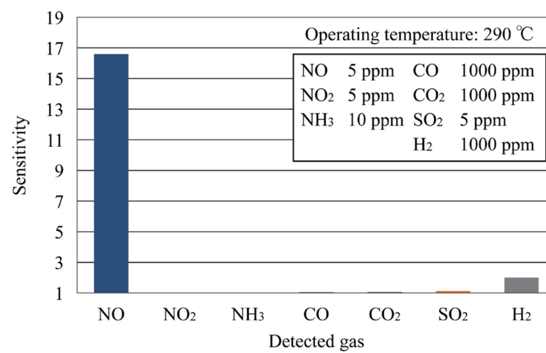

Fig. 9. (Color online) Gas selectivity of double-layered gas sensor with interspaces.

$$S = \frac{R_a}{R_g} \tag{2}$$

The sensitivity to NO_2, NH_3, CO, CO_2, and SO_2 gases was very low. It was slightly higher to hydrogen. However, the sensitivity to 5 ppm NO gas was much higher than that to 1000 ppm hydrogen. Therefore, the selectivity to NO gas was satisfactory.

3.6 Proposed mechanism of nitric oxide gas sensing

The mechanism of NO gas sensing is proposed and it is shown why the multilayered sensors with interspaces are sensitive and selective to NO gas. The gap between the sensing films is ca. 20 nm, which is much shorter than the mean free path (ca. 100 nm) of NO, O_2, and N_2 gases. Thus, these gas molecules inside interspaces collide with the upper and lower sensing films many times before colliding with other molecules. Some NO and O_2 molecules adsorb on the surface of the sensing films because they are both chemically active. When they desorb from the surface, a part of them can be activated. The activated species easily adsorb on the surface again and tend to become chemisorbed species such as NO^- and O_2^- on the surface by accepting electrons from the sensing film as shown below.

$$NO + e^- \rightarrow NO^- \tag{3}$$

$$O_2 + e^- \rightarrow O_2^- \quad (4)$$

Some O_2 molecules may be chemisorbed as O^- and O^{2-} depending on the temperature.[17] Although the reaction such as Eq. (4) occurs on the ordinary surface of the sensing film without interspaces, the reaction is promoted by the increased number of collisions with the sensing films and thus the resultant O_2^- species increase in number for the multilayered films with interspaces. Thus, the reaction of NO and O_2^- species is accelerated on the surface compared with that on the ordinary surface as follows.

$$2NO + O_2^- + e^- \rightarrow 2NO_2^- \quad (5)$$

This reaction is associated with the acceptance of more electrons from the sensing film, decreasing the electron concentration of the film and thus increasing the sensor resistance. This is possibly the reason why the sensitivity to NO is high for the multilayered sensor with interspaces.

Ag doping into WO_3 has been reported to be effective in increasing the sensitivity to NO.[13,14] However, the microscopic structures of the sensing materials are different from that in this study. In this study, Ag atoms on the sensing surface promote O_2 adsorption and hence chemisorbed species such as O_2^- increase in number as a result of the reaction shown in Eq. (4). Thus, Ag doping into the WO_3-based film successfully enhances the sensitivity to NO. Figure 10 illustrates the proposed model of NO gas sensing. NO gas reacts with chemisorbed oxygen species on the surface of Ag atoms on the WO_3-based film, accepting electrons from the film as shown in Eq. (5). Ag is also doped inside the WO_3 film. However, the Ag atoms that appear on the surface are active, enhancing the chemisorption of oxygen atoms.

NO_2, SO_2, and CO_2 do not react with chemisorbed oxygen species. This may be the reason why the sensors do not exhibit high sensitivity to these gases. CO and H_2 react with chemisorbed oxygen species; the sensors show a slight sensitivity to these gases. However, the reaction rates of CO and H_2 are not much higher than that of NO, which is a type of radical and chemically active. Therefore, the sensors are sensitive and selective to NO gas.

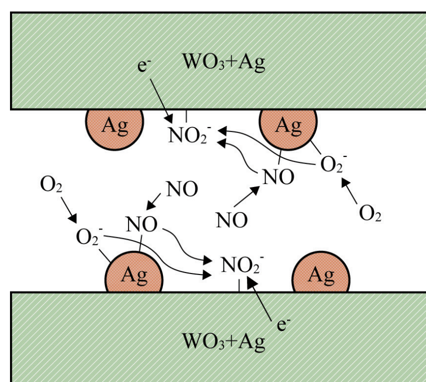

Fig. 10. (Color online) Proposed mechanism of NO gas sensing.

4. Conclusions

Novel NO gas sensors were developed using multilayered WO_3-based thin films with interspaces. Ag doping into the WO_3 thin film was effective in increasing the sensitivity to NO. A multilayered thin film with interspaces successfully enhanced both sensitivity and selectivity to NO. The developed sensor with quadruple-sensing layers can detect as low as 0.5 ppm NO gas with good selectivity at an operating temperature of 290 °C. A model was proposed to explain the sensing mechanism of NO gas. The response and recovery times were 81 and 138 s, respectively, for the double-layered sensor, while its sensitivity was lower than that of the quadruple-layered sensor. The sensors are thus promising as a portable and inexpensive NO sensing device in various application fields such as environmental monitoring and health diagnosis.

An even higher sensitivity is required to determine the NO gas concentration contained in exhaled breath. The device configurations, materials, and additives have to be optimized in future work.

References

1 B. T. Marquis and J. F. Vetelino: Sens. Actuators, B **77** (2001) 100.
2 G. Ko, H. Y. Kim, J. Ahn, Y. M. Park, K. Y. Lee, and J. Kim: Curr. Appl. Phys. **10** (2010) 1002.
3 N. Miura, H. Kurosawa, M. Hasei, G. Lu, and N. Yamazoe: Solid State Ionics **86** (1996) 1069.
4 N. F. Szabo and P. K. Dutta: Solid State Ionics **171** (2004) 183.
5 A. Dutta, N. Kaabbuathong, M. L. Grilli, E. Di Bartolomeo, and E. Traversa: J. Electrochem. Soc. **150** (2003) H33.
6 J. Yoo, S. Chatterjee, and E. D. Wachsman: Sens. Actuators, B **122** (2007) 644.
7 E. Di Bartolomeo, N. Kaabbuathong, M. L. Grilli, and E. Traversa: Solid State Ionics **171** (2004) 173.
8 N. Yamazoe and N. Miura: New Approaches in the Design of Gas Sensors: Gas Sensor (Kluwer, Dordrecht, 1992) p. 1.
9 S. C. Moulzolf, S. Ding, and R. J. Lad: Sens. Actuators, B **77** (2001) 375.
10 X. Wang, N. Miura, and N. Yamazoe: Sens. Actuators, B **66** (2000) 74.
11 M. Akiyama, J. Tamaki, N. Miura, and N. Yamazoe: Chem. Lett. **20** (1991) 1611.
12 Z. Cai, H. Li, X. Yang, and X. Guo: Sens. Actuators, B **219** (2015) 346.
13 L. Chen and S. C. Tsang: Sens. Actuators, B **89** (2003) 68.
14 D. Chen, L. Yin, L. Ge, B. Fan, R. Zhang, J. Sun, and G. Shao: Sens. Actuators, B **185** (2013) 445.
15 K. Sawaide, T. Yamada, and K. Hara: Proc. 14th IMCS (2012) 546.
16 T. Hiwatari and K. Hara: IEEJ Trans. **118-E** (1998) 136.
17 G. Heiland and D. Kohl: Chemical Sensor Technology Vol. 1 (Kodansha Ltd., Tokyo and Elsevier, Amsterdam, 1988) p. 15.